

AN INTERFACE CAPTURING APPROACH WITH BOUNDED CONTINUOUS RENORMALIZATION FOR FREE SURFACE FLOWS

Laura Battaglia, Mario A. Storti and Jorge D'Elía

Centro Internacional de Métodos Computacionales en Ingeniería (CIMEC)

Instituto de Desarrollo Tecnológico para la Industria Química (INTEC)

Universidad Nacional del Litoral - CONICET

Güemes 3450, 3000-Santa Fe, Argentina, e-mail: lbattaglia@santafe-conicet.gob.ar

web page: <http://www.cimec.org.ar>

Keywords: fluid mechanics, free surface, interface-capturing, level-set method, bounded continuous renormalization.

Abstract. An interface capturing approach based on a level set function for simulating transient two-fluid viscous incompressible flows is presented. Each fluid is indicated with a positive or negative value of the level set function, corresponding to a liquid phase and a gaseous one, respectively, in the particular case of free surface flows, where the interface is represented by the zero level set. The methodology is numerically solved in three stages: the first one is a two-fluid Navier–Stokes solver, followed by an advective step for transporting the level set function. The third stage consist in the level set function correction through a bounded renormalization with continuous penalization which keeps certain properties over the transition between fluids. The proposed procedure, and particularly the renormalization stage, are evaluated in different typical cases: advection-renormalization examples and fluid-advection-renormalization problems.

1 INTRODUCTION

Fluid flows with interfaces are present in several disciplines, such as chemical, mechanical or civil engineering. Particularly, Free Surface (FS) flows constitute a subset of that kind of flows, where there are two fluids involved, but the lighter of them has little influence over the other due to its negligible viscosity. Among these last flows, there are some that are not sensitive to the surface tension effects, such as sloshing in tanks for transporting liquids, open channel flows, spillways, FS flow around rigid objects, or simply tank filling. The numerical resolution of this kind of transient problems motivate the proposal presented here, under the hypothesis of Newtonian, viscous and incompressible fluid flow.

There are two main approaches for the computation of FS flows: interface tracking or interface capturing (Shyy et al., 1996). The first approach consist in following explicitly the FS because it is defined over discrete entities such as nodes or elements of a Finite Element Method (FEM) mesh. The interface capturing strategy generally counts on a fixed or Eulerian mesh where the FS crosses the elements and must be captured by an additional component, like a new variable or a fluid fraction, allowing topological changes as breaking up or merging of the interface.

Interface tracking methods can be purely Lagrangian, as particle methods (Idelsohn et al., 2004), or can be developed as Arbitrary Lagrangian-Eulerian (ALE) approaches (Hughes et al., 1981; Huerta and Liu, 1988; Rabier and Medale, 2003), where the FS is defined, in general, as a boundary of the domain of analysis, which in turn is deformed by the interface displacement in such a way that the mesh must be deformed or regenerated. The ALE approaches are usually more precise regarding FS displacements, especially for small deformations.

Regarding interface tracking, a FEM-ALE strategy was presented in previous works (Battaglia et al., 2006, 2007), but the proposal was limited to flows without FS breaking up or other cases where the uniqueness of the interface is verified.

By the other side, classical methods for interface capturing are Volume of Fluid (VOF) (Hirt and Nichols, 1981; Scardovelli and Zaleski, 1999) and Level Set (LS) (Osher and Sethian, 1988; Sethian, 1995). Roughly speaking, VOF consist on using a fluid fraction F on each cell, which is $F = 0$ in gaseous regions, $F = 1$ in liquid ones and $0 < F < 1$ where cells are crossed by the interface, which is reconstructed by algorithms of strong geometrical base. By the other side, LS approximations count on an additional continuous variable that is transported by an advective expression, as will be explained below.

In this work, a LS interface capturing approach is presented, for analyzing a two-fluid isothermal flow inside a unique domain, where the phases are considered Newtonian, viscous and incompressible. In this approximation, each fluid is indicated with a positive or negative value of the LS function ϕ , being $\phi > 1$ for the liquid phase and $\phi < 0$ for the gaseous one in the case of FS flows, while for the interface is $\phi = 0$. The function ϕ is defined over the whole domain of analysis, is continuous across the FS $\phi = 0$ and is used for indicating the fluid properties when the flow is numerically solved. Part of this proposal was introduced in Battaglia et al. (2008), and was improved in Battaglia (2009).

The algorithm proposed consist of three stages solved alternately each time step: the first one solves the flow problem over the domain considering the presence of two fluids; the second one determines the transport of the ϕ function due to the fluid velocities, and the last one, which can be done every certain number of temporal steps, keeps the regularity of the LS function ϕ principally in the neighbourhood of the interface, as presented in Battaglia (2009). Each of the stages is solved numerically by FEM, through the use of some libraries from the PETSc-

FEM (2009) code, which is based on the Portable Extensible Toolkit for Scientific Computation (PETSc) (Balay et al., 2005) libraries for parallel computing and the Message Passing Interface (MPI, 2009).

The methodology proposed here is evaluated for two kinds of typical problems found in literature: advection-renormalization tests and fluid-advection-renormalization tests. Advection-renormalization problems are used for the evaluation of the renormalization procedure, and the introduction of the fluid stage allows the analysis of the capabilities of the procedure for solving free surface problems.

2 GOVERNING EQUATIONS

As mentioned before, the fluid flow problem is solved through a three stages algorithm, where each of them consist in solving by FEM the spatial part of a Partial Differential Equations (PDEs) system, described in the following sections. For both instances, fluid flow and LS function advection, temporal integration is made by the trapezoidal rule with parameter α , being $\alpha = 1$ for the Backward Euler method and $\alpha = 0.5$ for the Crank-Nicolson one.

2.1 Fluid state

The first system of PDEs is the Navier–Stokes (NS) one, which is proposed for the case of two incompressible and immiscible fluid flows in the Ω domain for time $t \in [0, T]$, in the following way:

$$\begin{aligned} \rho(\phi(\mathbf{x}, t)) (\partial_t \mathbf{v} + \mathbf{v} \cdot \nabla \mathbf{v} - \mathbf{f}) - \nabla \cdot \boldsymbol{\sigma} &= 0 ; \\ \nabla \cdot \mathbf{v} &= 0 ; \end{aligned} \quad (1)$$

where $\mathbf{x} \in \Omega$ is the position vector, \mathbf{v} is the fluid velocity, \mathbf{f} the body force, $\rho(\phi(\mathbf{x}, t))$ the fluid density, $\partial_t(\dots) = \partial(\dots)/\partial t$ indicates the partial time derivative and ϕ is the LS function.

The fluid stress tensor $\boldsymbol{\sigma}$ can be decomposed in an isotropic $-p\mathbf{I}$ part and a deviatoric one \mathbf{T} ,

$$\boldsymbol{\sigma} = -p\mathbf{I} + \mathbf{T} ; \quad (2)$$

being p the pressure, \mathbf{I} the identity tensor and \mathbf{T} the viscous forces tensor, which is a function of the strain rate tensor $\boldsymbol{\epsilon}$ determined as

$$\begin{aligned} \mathbf{T} &= 2 \mu(\phi(\mathbf{x}, t)) \boldsymbol{\epsilon} ; \\ \boldsymbol{\epsilon} &= \frac{1}{2} \left[\nabla \mathbf{v} + (\nabla \mathbf{v})^T \right] ; \end{aligned} \quad (3)$$

for Newtonian fluids. In the last expression, $(\dots)^T$ indicates transposition and $\mu = \mu(\phi(\mathbf{x}, t))$ is the dynamic viscosity.

The fluid density and viscosity depend on both the position \mathbf{x} and the evaluation time t because of the multiphase proposal, which is given by the LS function ϕ . The function ϕ , defined over the whole domain Ω , indicates the region of Ω which is occupied by one or another fluid (Sussman and Smereka, 1997), such that

$$\phi(\mathbf{x}, t) \begin{cases} > 0 & \text{if } \mathbf{x} \in \Omega_l ; \\ = 0 & \text{if } \mathbf{x} \in \Gamma_{FS} ; \\ < 0 & \text{if } \mathbf{x} \in \Omega_g ; \end{cases} \quad (4)$$

where the subdomain Ω_l corresponds to the liquid phase, Ω_g is the gaseous one and $\Omega = \Omega_l \cup \Omega_g$ is verified. The subindex adopted are such that l and g correspond to the liquid and the gaseous

regions respectively, considering that the present proposal is oriented to the resolution of FS flows. Particularly, the FS is defined as the set

$$\Gamma_{\text{FS}} = \{\mathbf{x} | \phi(\mathbf{x}, t) = 0\}. \quad (5)$$

Regarding the method proposed for the renormalization of ϕ in Sec. 2.3, the LS function will verify $-1 \leq \phi \leq 1$, with a smooth continuous transition between these values.

Then, the fluid properties for Eqs. (1) and (3), as in most LS procedures (Sussman and Smereka, 1997), are given as functions of the ϕ values,

$$\begin{aligned} \rho(\phi) &= \frac{1}{2} \left[\left(1 + \tilde{H}(\phi)\right) \rho_l + \left(1 - \tilde{H}(\phi)\right) \rho_g \right]; \\ \mu(\phi) &= \frac{1}{2} \left[\left(1 + \tilde{H}(\phi)\right) \mu_l + \left(1 - \tilde{H}(\phi)\right) \mu_g \right]. \end{aligned} \quad (6)$$

where $\tilde{H}(\phi)$ is determined through:

$$\tilde{H}(\phi) = \tanh\left(\frac{\pi\phi}{\tilde{\varepsilon}}\right); \quad (7)$$

which is slightly different from other smeared out Heaviside $\tilde{H}(\phi)$ functions found in the literature (Sussman and Smereka, 1997; Olsson and Kreiss, 2005). In this case, for $|\phi| \rightarrow \tilde{\varepsilon}$ is $\tilde{H}(\phi) \rightarrow 1$, which reduces the length of the transition in the fluid properties in comparison to the transition between $\phi = -1$ and $\phi = 1$. For all the cases, $\tilde{\varepsilon} = 0.5$ was adopted, which reduces the transition length in about 70%. It must be noticed that the reduction of this strip is made for providing a more precise fluid properties values for the NS solver, leaving a wider strip for the advection step in order to transport ϕ in a more precise way.

Boundary conditions for \mathbf{v} in Eq. (1) are given over the solid boundaries Γ_{wall} , in all the problems proposed here. In the case of the pressure, $p = 0$ is proposed for the top of the domain.

The resolution is obtained through the NS solver from the PETSc-FEM libraries, considering linear elements with the same interpolation for velocity and pressure fields, stabilized with streamline upwind/Petrov-Galerkin (SUPG) (Brooks and Hughes, 1982) and pressure stabilizing/Petrov-Galerkin (PSPG) (Tezduyar et al., 1992).

2.2 Level set function advection

A simultaneous advection and renormalization procedure was presented in a previous work (Battaglia et al., 2008), but further tests showed that some requirements over the solution were not verified, such as keeping the transition strip with constant width (Battaglia, 2009). Because of that, a different strategy was implemented, which consist in an advection step for transporting ϕ followed by a renormalization step described in Sec. 2.3.

The transport of the LS function ϕ over the domain Ω is generated by the velocity field \mathbf{v} determined by solving the NS equations, and can be written as follows,

$$\partial_t \phi + \mathbf{v} \cdot \nabla \phi = 0; \quad (8)$$

while boundary conditions are given by

$$\phi = \bar{\phi} \quad \text{over} \quad \Gamma_{\text{in}}; \quad (9)$$

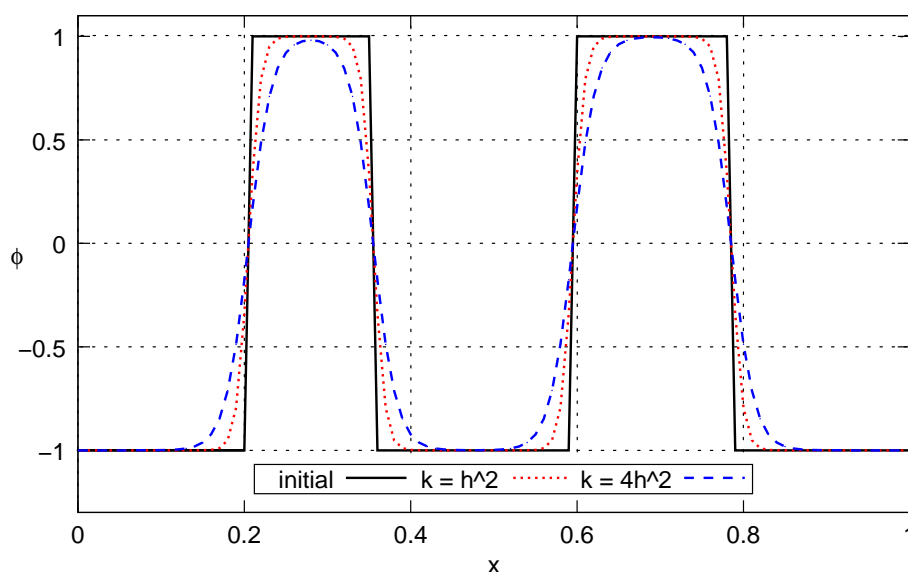


Figure 1: Artificial reaction-diffusion problem for renormalization of ϕ depending on the diffusion coefficient κ values.

i.e., in cases with inflow sections $\Gamma_{\text{in}} = \{\Gamma \mid \mathbf{v} \cdot \mathbf{n} < 0\}$. This advection procedure takes into account the transport of Γ_{FS} in a natural way. In some cases, periodic boundary conditions are considered.

The numerical resolution is made by the advective module of the PETSc-FEM program, which is denominated ADV in this work. This module count on the SUPG strategy for avoiding numerical instabilities because of the use of a central scheme as Galerkin for the resolution of the transport equation for the LS function ϕ .

2.3 Renormalization procedure

For a more complete discussion about the proposed renormalization, see Battaglia (2009). A similar proposal is given as part of the *Conservative Level Set Method* (Olsson and Kreiss, 2005; Olsson et al., 2007), although it does not count on a penalization term as in the present proposal.

The renormalization process is proposed as the resolution of a PDE system of equations by FEM, where the variable is ϕ . The operator, denominated Bounded Renormalization with Continuous Penalization (BRCP), is

$$\phi (\phi^2 - \phi_{\text{ref}}^2) - \kappa \Delta \phi + M (\check{H}(\phi) - \check{H}(\phi^0)) = 0; \quad (10)$$

being κ the diffusion parameter, M the penalization coefficient and ϕ_{ref} a reference value for the variable ϕ , adopted as $\phi_{\text{ref}} = 1$, while ϕ^0 is the LS function initial value for the renormalization step provided by ADV. The coefficient M is non-dimensional and should be adopted as $O(10^{n_d+2})$, with n_d the number of spatial dimensions involved. The diffusion parameter κ is given in longitude² units, and is related to a typical mesh element size h , usually from h^2 to $(3h)^2$, depending on the FS behaviour: a lower κ provides a thinner transition.

The penalizing function $\check{H}(\phi)$ is adopted as the continuous expression

$$\check{H}(\phi) = \tanh(2\pi\phi); \quad (11)$$

which is also a smeared out Heaviside function, as the one given in Eq. (7).

As an example of how Eq. (10) works over the ϕ field, the effect of part of this equation will be analyzed over a one-dimensional domain $0 \leq x \leq L$,

$$\phi (\phi^2 - \phi_{\text{ref}}^2) - \kappa \Delta \phi = 0; \quad (12)$$

which is a reaction-diffusion-like equation. If the laplacian term is neglected, i.e. $\kappa = 0$, and the level set function takes values $\phi = \pm \phi_{\text{ref}} = \pm 1$, which are the stable roots of Eq. (12) according to the stability criteria for the fixed point method, then, there are infinite solutions continuous by pieces for the reactive term, where each segment is rect and takes one of the roots values, as plot in Fig. 1 for $\kappa = 0$. If the Laplacian term is reintroduced, the resolution of Eq. (12) become a continuous function with smooth transition between $\phi = \pm \phi_{\text{ref}}$, the stable roots, see Fig. 1. It is verified that a larger value of the diffusion parameter lead to a wider transition between $\pm \phi_{\text{ref}}$.

The last term of Eq. (10), or penalizing term, allows taking into account the known values ϕ^0 , i.e. those determined in the advection step. The aim of this term is avoiding the displacement of the FS, represented by $\phi = 0$, by weighting $\check{H}(\phi) - \check{H}(\phi^0)$. Other authors proposed penalty parameters for preserving the interface position, as in the Edge-Tracked Interface Locator Technique (ETILT) Tezduyar (2006); Cruchaga et al. (2007) method.

The regions placed far from the interface are not affected by the renormalization process because when $\phi \approx \phi_{\text{ref}}$, all the three terms in Eq. (10) tends to zero. On the other hand, the higher influence of the operator is registered in the neighbourhood of $\phi = 0$, where the loss of precision in the FS position and mass loss is registered (Mut et al., 2006; Cruchaga et al., 2007).

Regarding the selection of the free parameter values, κ and M , in cases where FS would suffer breaking up or would fold several times it is convenient adopting a low κ value and a high M one, because transitions should be thinner and M would avoid the disappearance of the drops.

The operator presented in Eq. (10) is numerically solved by FEM, taking as initial condition ϕ^0 the ϕ values transported by the previous advection step. Besides, the regularization can be applied each time step or every n_{reno} time steps.

3 NUMERICAL EXAMPLES

The numerical examples proposed are separated in two different sections, regarding the stages to be evaluated. The first problems proposed, incorporated in Sec. 3.1, are designed for evaluating the advection-renormalization strategy, avoiding the costs of the fluid flow resolution and proposing deformation fields hard to solve for these stages. The rest of the tests include the fluid flow step for typical FS problems, see Sec. 3.2, where the FEM results are compared to experimental data.

3.1 Advection-Renormalization problems

3.1.1 Vortex 2D

A typical test case for the advection-renormalization strategy consist in solving the deformation of a disk of radius $r = 0.15$ m with $\phi > 1$ inside, centered in $(x_c, y_c) = (0.50, 0.75)$ m for a square domain with side length of 1 m, i.e. x and y -coordinates vary from 0 to 1 m. This disk, represented exactly by $\phi = 0$, is submitted to a velocity field defined by the stream function Ξ ,

$$\Xi = -\frac{1}{\pi} \sin^2(\pi x) \sin^2(\pi y); \quad (13)$$

from which the velocity field components over the domain is given by the following components,

$$v_x = -\frac{\partial \Xi}{\partial y} = -\sin(2\pi y) \sin^2(\pi x); \quad (14)$$

$$v_y = +\frac{\partial \Xi}{\partial x} = \sin(2\pi x) \sin^2(\pi y); \quad (15)$$

This example, or slightly different ones, is taken as reference for evaluating the performance of several interface-capturing methods such as LS (Di Pietro et al., 2006; Enright et al., 2002; Gois et al., 2008; Herrmann, 2008; Olsson and Kreiss, 2005) or VOF (Elias and Coutinho, 2007).

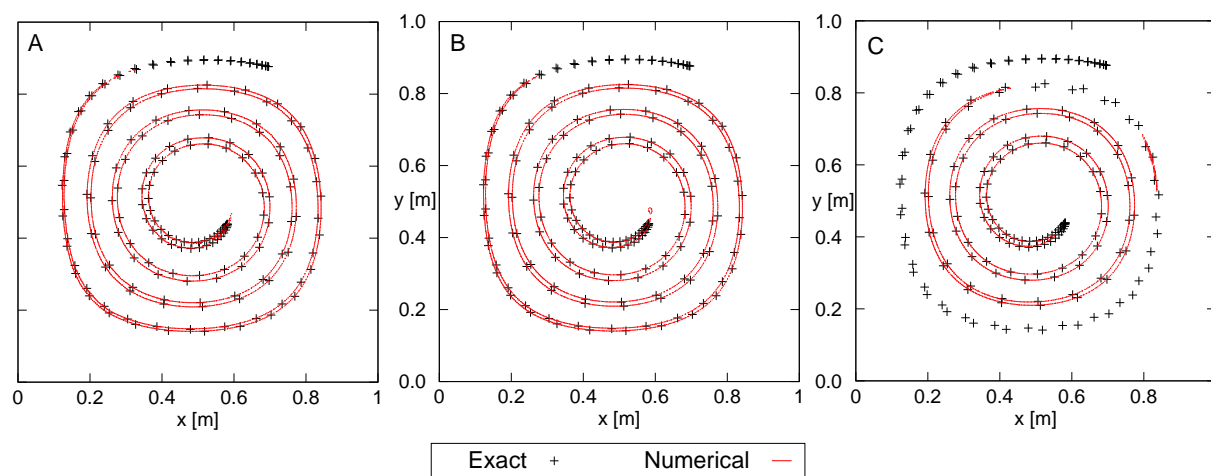


Figure 2: Curves of $\phi = 0$ in $t_f = 5$ s for the 2D vortex, considering advection (A), advection and renormalization (B), and advection stabilized with SUPG (C).

The selected variant is the application of the velocity field from Eqs. (14,15) up to a final time $t_f = 5$ s. The results obtained by the FEM advection-renormalization strategy were compared to the position of some particles initially disposed over the contour of the circle and transported by the given velocity field. In this way, the comparison between the FEM resolution and the theoretical deformation allows the evaluation of the ability of the method for reproducing the deformation and the capabilities related to area preservation.

The problem was numerically solved in three different ways,

- A. advection without numerical stabilization, for a uniform tessellation of around 131000 linear triangular elements, with 256 elements in each boundary side;
- B. non-stabilized advection and BRCP every $n_{\text{reno}} = 10$ time steps over the same discretization as in A, adopting diffusivity $\kappa = 2h^2 = 3.06 \times 10^{-5} \text{ m}^2$ and penalization $M = 10000$;
- C. as in A, with SUPG stabilization.

In all the cases, the Courant number was taken as $Co = 0.5$, which lead to a time step $\Delta t = 1.95 \times 10^{-3}$ s in all the three cases.

The interface identified with $\phi = 0$ obtained in cases A, B and C, all of them through FEM, is represented in Fig. 2 with continuous trace, while the reference particles are plot with crosses. This figure shows little difference between the curves obtained in A and B, and an important loss of the positive area ($\phi > 0$) in C.

In spite of the small differences between the results of A and B, the resolution in B shows around 0.5% of mass loss, while in case A the positive area is diminished in 2.5%, approximately. It is clear from Fig. 2 that the mass loss in C is much higher than those mentioned above: 26%.

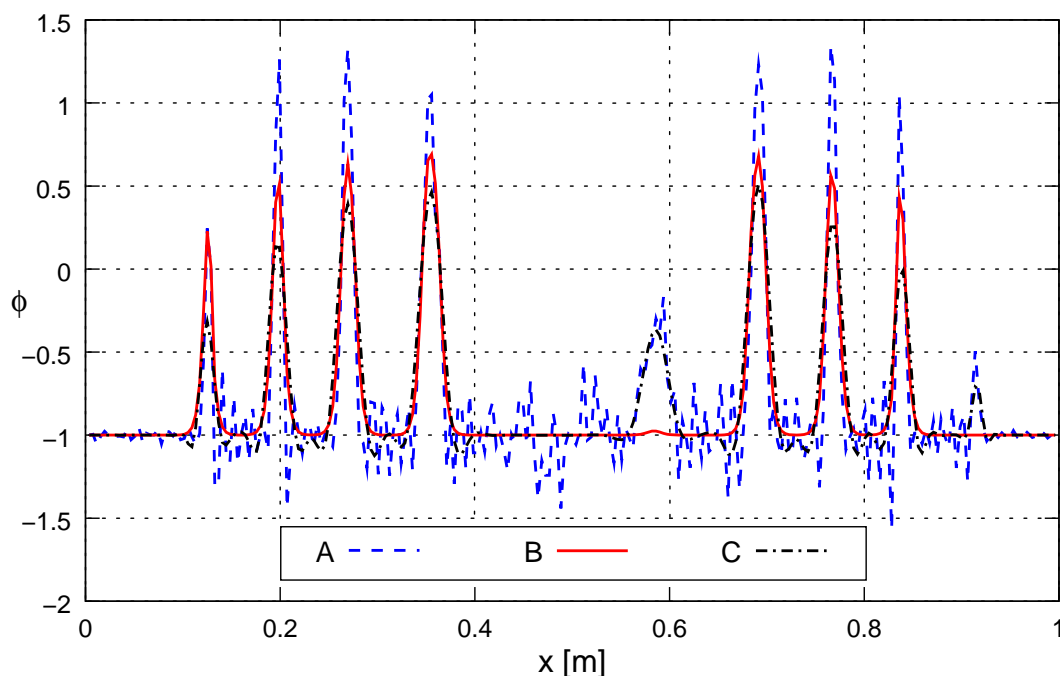


Figure 3: Section in $y = 0.5$ m for the 2D vortex problem in $t_f = 5$ s for pure advection (A), advection and renormalization (B) and advection stabilized with SUPG (C).

From another point of view, the analysis of the LS function profile along a section in $y = 0.5$ m shows the differences between the advection solution A with numerical instabilities, a smooth advection-renormalization solution B without numerical stabilization in the advection stage, and a stabilized advection solution C, where the use of SUPG lead to the disappearance of the positive area, i.e. $\phi > 0$ region, due to the diffusion introduced by such stabilization method.

3.1.2 Vortex 3D

A 3D extension of the two-dimensional vortex of Sec. 3.1.1 was proposed by LeVeque (1996) and considered later for several authors like Elias and Coutinho (2007); Enright et al. (2002); Gois et al. (2008), among others.

The example consist in the deformation of a sphere with radius $r_e = 0.15$ m defined by the LS corresponding to $\phi = 0$, centered in coordinates (0.35, 0.35, 0.35) m of the unit cube, submitted to the following velocity field,

$$\begin{cases} v_x &= 2 \sin^2(\pi x) \sin(2\pi y) \sin(2\pi z) \cos\left(\frac{\pi t}{T_e}\right); \\ v_y &= -\sin(2\pi x) \sin^2(\pi y) \sin(2\pi z) \cos\left(\frac{\pi t}{T_e}\right); \\ v_z &= -\sin(2\pi x) \sin(2\pi y) \sin^2(\pi z) \cos\left(\frac{\pi t}{T_e}\right); \end{cases} \quad (16)$$

where the period is $T_e = 3$ s. The proposed time evolution for the velocity field generates two contra-rotating vortices that produce a deformation of the positive region of ϕ between $t = 0$ and $t = 1.5$ s, resulting in a thin, squashed form. Then, the velocity field is inverted and the sphere should be recovered in $t = 3$ s.

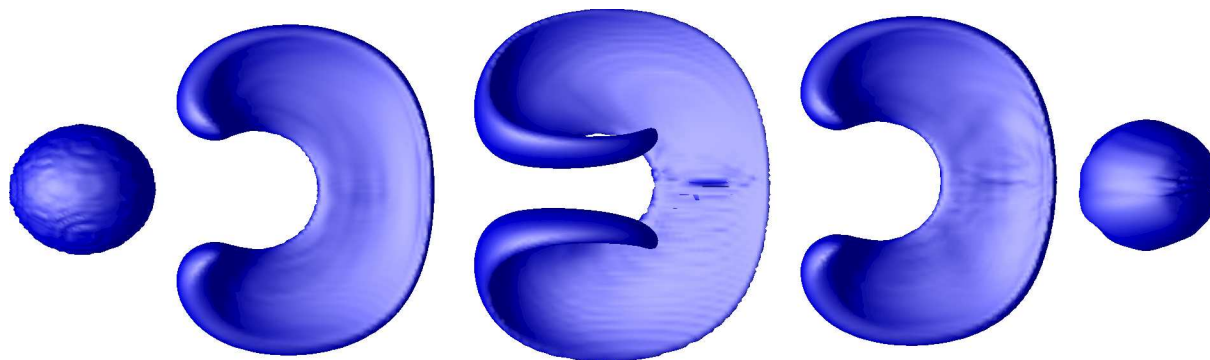


Figure 4: Surface defined by $\phi = 0$ for the 3D vortex solved with advection and BRCP, for times 0.02 s, 0.76 s, 1.50 s, 2.25 s and 3.00 s from left to right, respectively.

The FEM simulation was made over a 128^3 hexahedral elements regular mesh, with $n_{\text{reno}} = 10$ time steps, $\Delta t = 0.00195$ s, $\kappa = 6h^2 = 3.66 \times 10^{-4}$ m² and $M = 100000$. Figure 4 shows the evolution of the interface $\phi = 0$ in different time instants. Because of the periodic character of the velocity field, the shapes registered in $t = 3$ s and $t = 0$ should be equal, as well as $t = 2.25$ s and $t = 0.76$ s.

3.2 Fluid flow-Advection-Renormalization problems

3.2.1 Collapse of a liquid column in 2D

This example, also known as the *dam-break problem* is a classic water column collapse test for interface-capturing methods (Cruchaga et al., 2007; Elias and Coutinho, 2007; Marchandise and Remacle, 2006; Tang et al., 2008). In this problem, a two dimensional water column breaks up when is instantaneously liberated inside an air atmosphere. For this problem, there are experimental results which allow the validation of numerical codes (Cruchaga et al., 2007; Martin and Moyce, 1952).

The geometrical data for this example are referred to Fig. 5, where the domain Ω is sketched, counting on width $W_d = 0.228$ m and height $H_d = 0.228$ m, while the water column is defined by $W_c = 0.057$ m and $H_c = 0.114$ m, i.e. the aspect ratio is $r_a = H_c/W_c = 2$, as adopted by Martin and Moyce (1952) for the physical model.

The fluid properties are those corresponding to water in the liquid phase, and air in the gaseous one, being the density $\rho_l = 1000$ kg/m³ and the dynamic viscosity $\mu_l = 1.0 \times 10^{-3}$ kg/(m s) for the liquid, and $\rho_g = 1$ kg/m³ and $\mu_g = 1.0 \times 10^{-5}$ kg/(m s) for the gas.

The boundary conditions adopted for the fluid problem are perfect slip over the whole domain contour, as indicated in Fig. 5, which means $\mathbf{v} \cdot \mathbf{n} = 0$, with \mathbf{n} the vector normal to the contour, and the pressure is given over the top of the box as $p = 0$. The advection problem to be solved by the ADV module of PETSc-FEM do not require boundary conditions because there are not inflow sections in Ω .

As both of the fluids are at rest at the beginning of the study, the initial velocity field is $\mathbf{v}_0 = \mathbf{0}$ in the NS and ADV problems, and the LS function field is defined in such a way that the nodes corresponding to the water column verify $0 < \phi \leq 1$, and the rest of them are comprised in

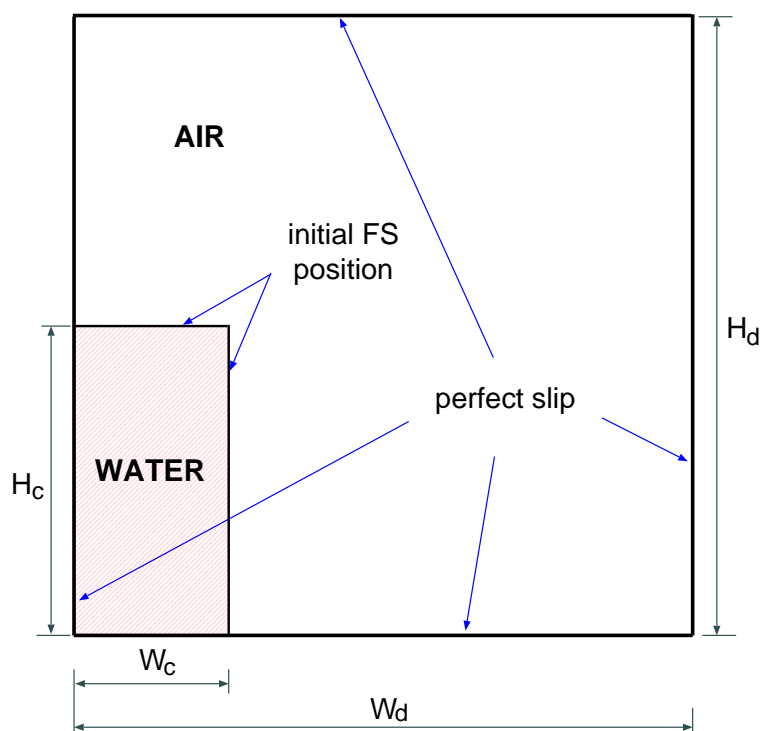


Figure 5: Geometry for the problem of the collapse of a water column in 2D.

$-1 \leq \phi < 0$, taking into account that $\phi = 0$ indicates the initial FS position. Once the analysis is started, the water column is affected by the vertical gravity acceleration, $g = 9.81 \text{ m/s}^2$, and collapses.

The numerical simulation was performed up to a final time $t_f = 2.0 \text{ s}$ in 1000 time steps, with a time stepping of $\Delta t = 0.002 \text{ s}$ and implicit temporal integration for the NS and the ADV problems. The finite element mesh is composed by quadrangles of typical size $h \approx 0.0023 \text{ m}$, with approximately 10200 nodes. This grid is structured, and was employed for the resolution of the three instances proposed in the algorithm: the NS, ADV and BRCP solvers.

The parameters adopted for the BRCP instance are $\kappa = 2h^2 = 1.04 \times 10^{-5} \text{ m}^2$ and $M = 10000$, with renormalization every $n_{\text{reno}} = 2$ time steps.

Figure 6 represents in the vertical axis the dimensionless front position $x_f(t^*)/W_c$, which is calculated as the quotient between the front position and the water column width W_c , as a function of the dimensionless time $t^* = t\sqrt{2g/W_c}$, for the numerical and the experimental results. In this figure, a displacement of the numerical curve from the experimental data is observed, but the slope of the FEM results matches the experimental one, that is, the advancing front velocity is well captured. The displacement mentioned before, which is about $\Delta t^* \approx 0.25$, could be attributed to the time needed for removing the lockgate during the experiment, that is not taken into account in the numerical simulation. Similar results were obtained by Cruchaga et al. (2007) and Elias and Coutinho (2007).

The dimensionless water height $h_c(t^*)/W_c$ over the left side of the domain as a function of the dimensionless time $t^* = t\sqrt{2g/W_c}$ is included in Fig. 7, taking as reference parameter for the dimensionless height the water column width W_c . As in Fig. 6, numerical simulation is slightly displaced from the experimental reference, around $\Delta t^* \approx 0.1$ faster, but the mean velocity is of about the same order than the one measured in the physical model (Martin and Moyce, 1952). This circumstance is also reported by other authors.

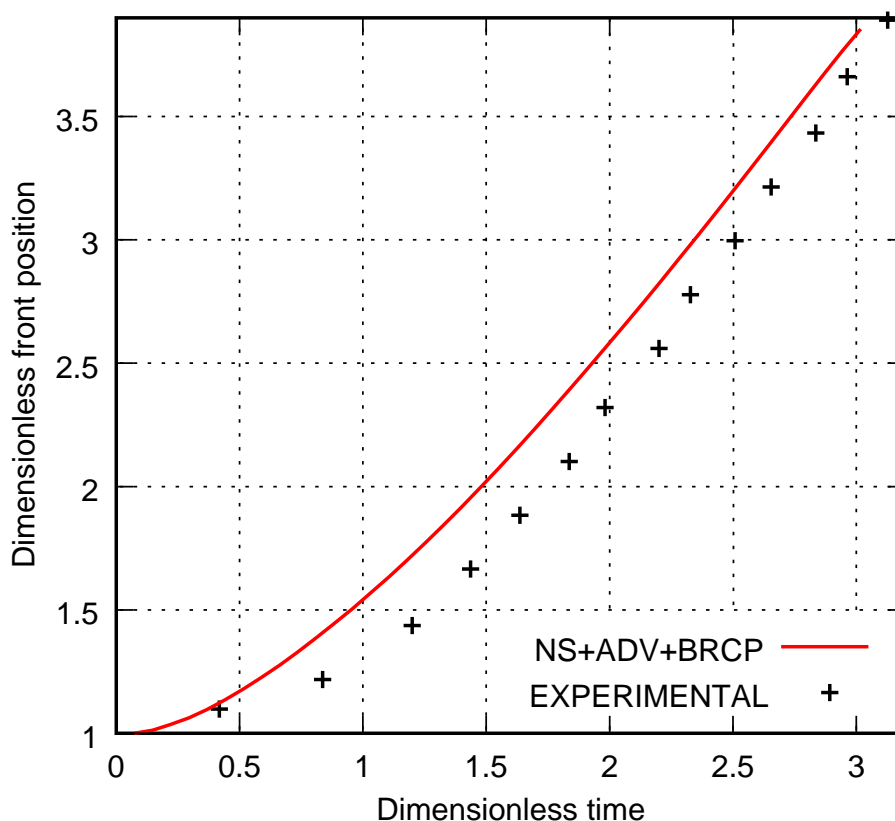


Figure 6: Dimensionless front position $x_f(t^*)/W_c$ versus dimensionless time $t^* = t\sqrt{2g/W_c}$ for the problem of the collapse of a water column in 2D: numerical results and experimental data.

Finally, Fig. 8 shows the FS position for some instants of the simulations, from early stages without FS breaking up, $t = 0.14$ s and $t = 0.28$ s, followed by stages with interface merging and air capture.

3.2.2 Collapse of a liquid column in 3D

As in the former case, the collapse of a cylindrical water column was studied experimentally by [Martin and Moyce \(1952\)](#). In this case, the computational simulation is performed over one fourth of the column, considering the domain represented in Fig. 9, and adopting boundary conditions in such a way that the axis symmetry of the experiment is kept. This test was also reproduced by other authors and several numerical methods ([Akin et al., 2007](#); [Cruchaga et al., 2008](#); [Tang et al., 2008](#)).

The domain geometry references are indicated in Fig. 9, which consist in a cube with edge length $b = 0.2284$ m. The water column is centered in the corner of plane coordinates $(x_1, x_2) = (0.2284, 0.2284)$ m and its radius and height are $r_0 = 0.0571$ m and $h_0 = 0.1142$ m, respectively, keeping an aspect ratio $r_a = 2$.

There is a gravity acceleration of $g = 9.81$ m/s² acting over the domain with $-x_3$ direction, which produces the collapse of the column. Density and dynamic viscosity parameters are $\rho_l = 1000$ kg/m³ and $\mu_l = 1.0 \times 10^{-3}$ kg/(m s) for the water, and in the case of the air $\rho_g = 1$ kg/m³ and $\mu_g = 1.0 \times 10^{-5}$ kg/(m s).

The simulation was performed over a structured mesh conformed by 50^3 hexahedra, each of them with edge length $h \approx 4.5 \times 10^{-3}$ m and the numerical simulation took 1000 time steps

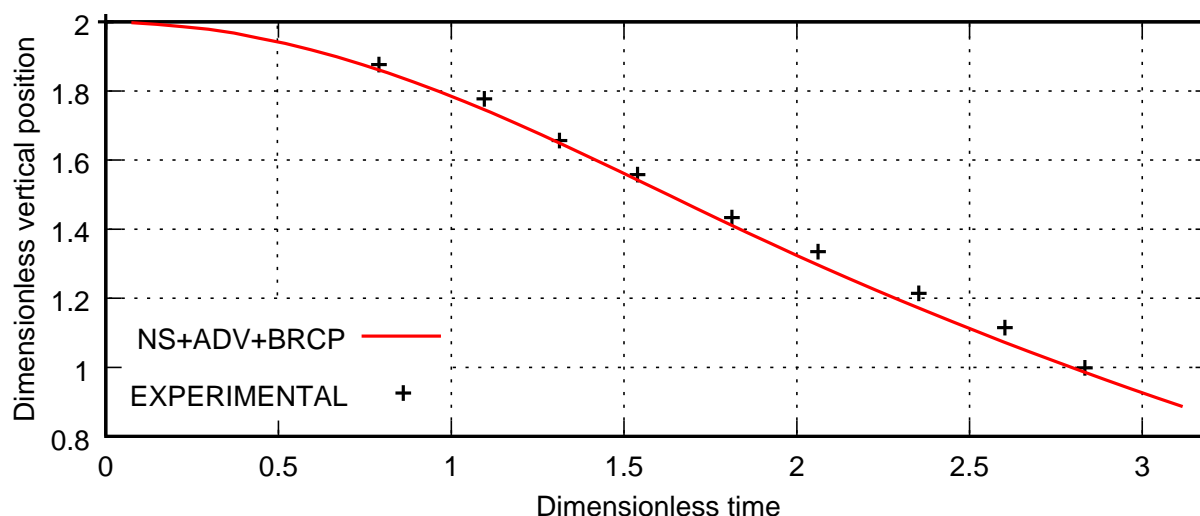


Figure 7: Dimensionless column height $h_c(t^*)/W_c$ versus dimensionless time $t^* = t\sqrt{2g/W_c}$ for the problem of the collapse of a water column in 2D: numerical results and experimental data.

of $\Delta t = 0.001$ s with implicit integration for NS and ADV. The renormalization stage was proposed with $\kappa = 2h^2 = 4.17 \times 10^{-5}$ m² and $M = 500000$. The boundary condition is perfect slip over all the domain walls for the NS stage, while there is no special consideration for ADV due to the absence of inflow sections.

The numerical results obtained by FEM are represented in Figs. 10 to 12. Experimental results (Martin and Moyce, 1952) provide data about the dimensionless front displacement $r_f(t^*)/r_0$, i.e. with respect to the initial ratio of the column r_0 , as a function of the dimensionless time $t^* = t\sqrt{2g/r_0}$. The numerical curve is superimposed to the experimental data in Fig. 10, where it is possible to see a good agreement between both results, especially after $t^* = 2.5$. In this case, there are no results from the physical model for the water column height, so only the results from the numerical model are represented in Fig. 11, considering the dimensionless descent $h_c(t^*)/r_0$ versus the dimensionless time t^* .

The collapse of the column sequence is drawn in Fig. 12, where it is possible to verify the symmetry of the movement.

4 CONCLUSIONS

A continuous operator, a Bounded Renormalization with Continuous Penalization (BRCP), was proposed for regularizing the LS function which is part of an interface-capturing approach for FS flow simulations, in two and three spatial dimensions.

Two kind of typical cases were solved by this procedure: advection-renormalization problems, where the BRCP strategy was strongly tested for particular flows in Sec. 3.1, and fluid-advection-renormalization examples with the purpose of evaluating the application of the algorithm in FS problems, Sec. 3.2.

The renormalization procedure shows a numerical stabilizing effect over the results provided by the advection stage avoiding, for instance, the use of SUPG stabilization in that instance.

Further work would be focused on including a wider range of boundary conditions for the NS and the ADV instances, such as those needed for the consideration of open boundaries such inflow or outflow sections. Besides, volume conservation should be taken into account for long time FS simulations, i.e., when the fluid flow solver is considered for the resolution.

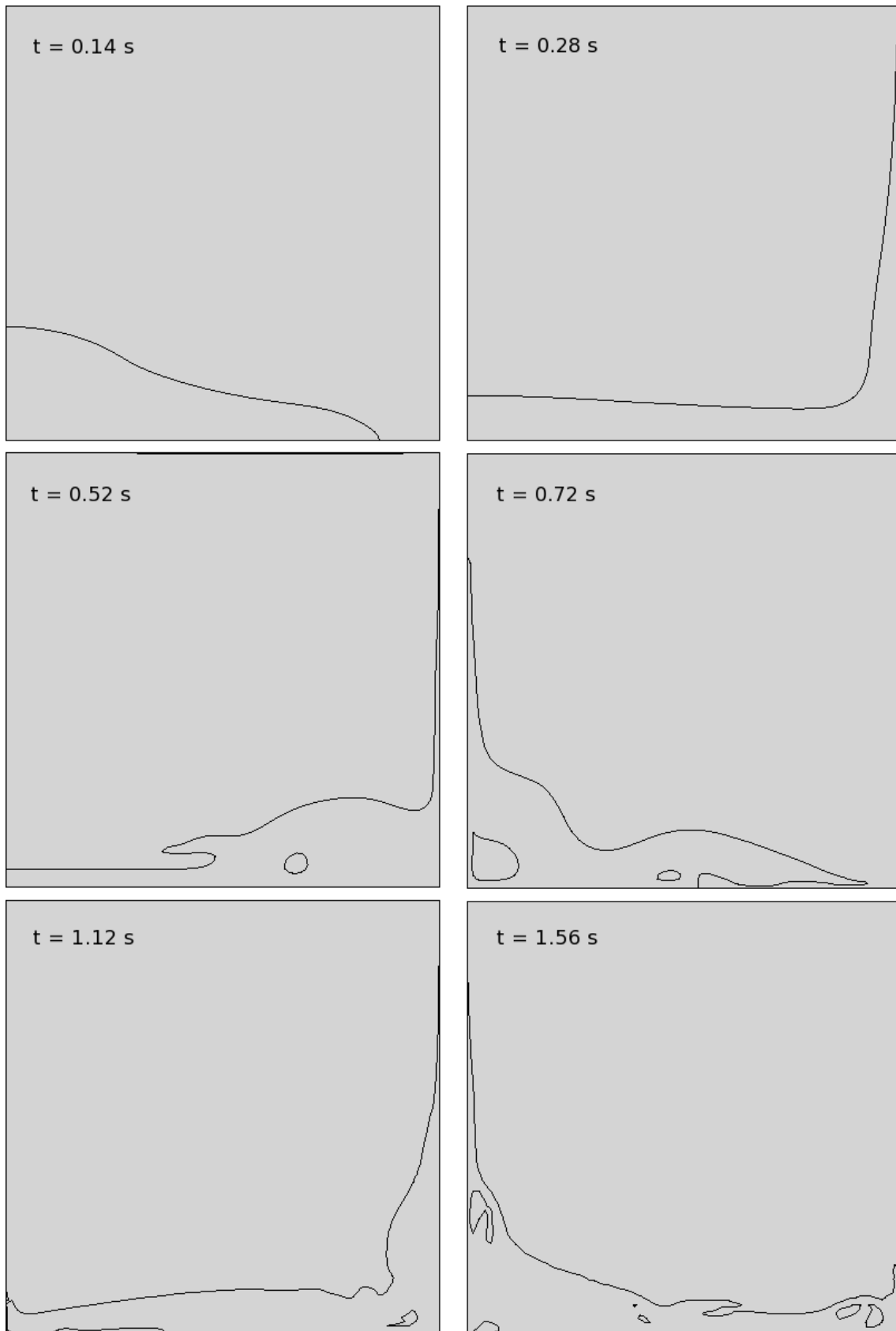


Figure 8: Free surface positions for different times in the 2D dam break problem.

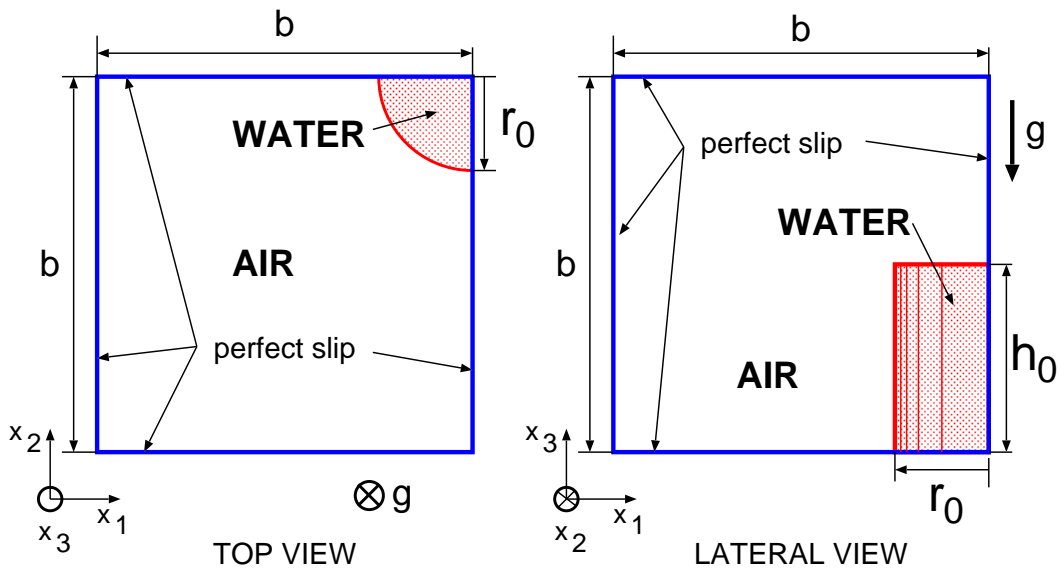


Figure 9: Geometry for the problem of the collapse of a cylindrical water column in 3D.

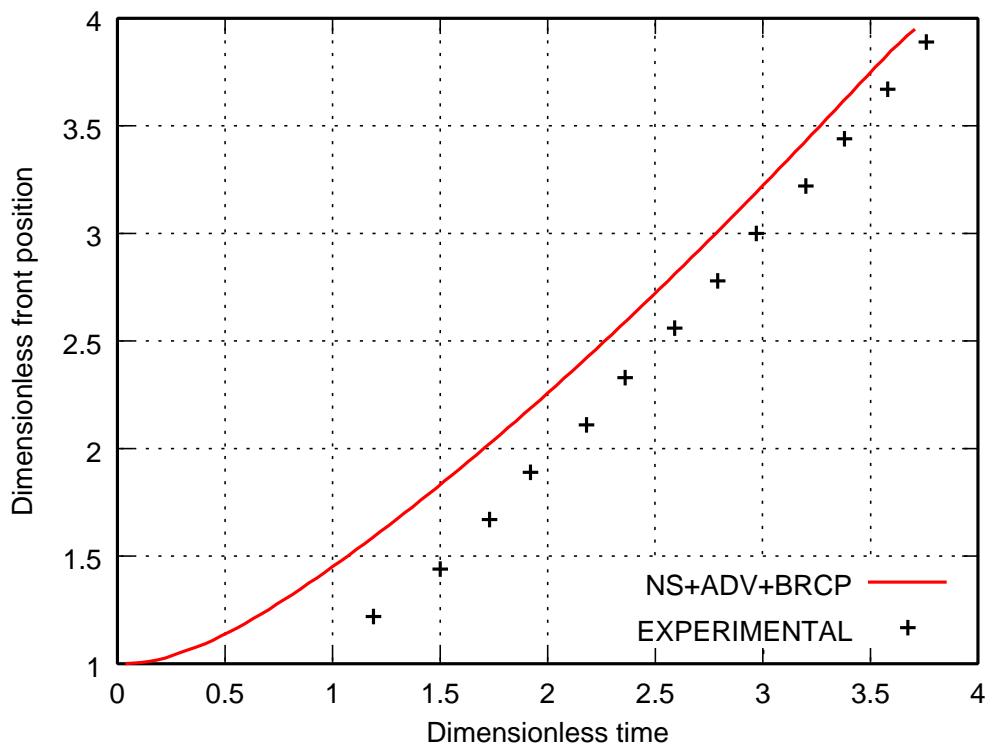


Figure 10: Dimensionless front position $r_f(t^*)/r_0$ versus dimensionless time $t^* = t\sqrt{2g/r_0}$ for the problem of the collapse of a cylindrical water column in 3D: numerical results and experimental data.

Acknowledgments This work has received financial support from Consejo Nacional de Investigaciones Científicas y Técnicas (CONICET, Argentina, grant PIP 5271/05), Universidad Nacional del Litoral (UNL, Argentina, grant CAI+D 2005-10-64/65, CAI+D 2009) and Agencia Nacional de Promoción Científica y Tecnológica (ANPCyT, Argentina, grants PICT 01141/2007, PICT 1506/2006), and was partially performed with the *Free Software Foundation GNU-Project* resources as GNU/Linux OS and GNU/Octave, as well as other Open Source

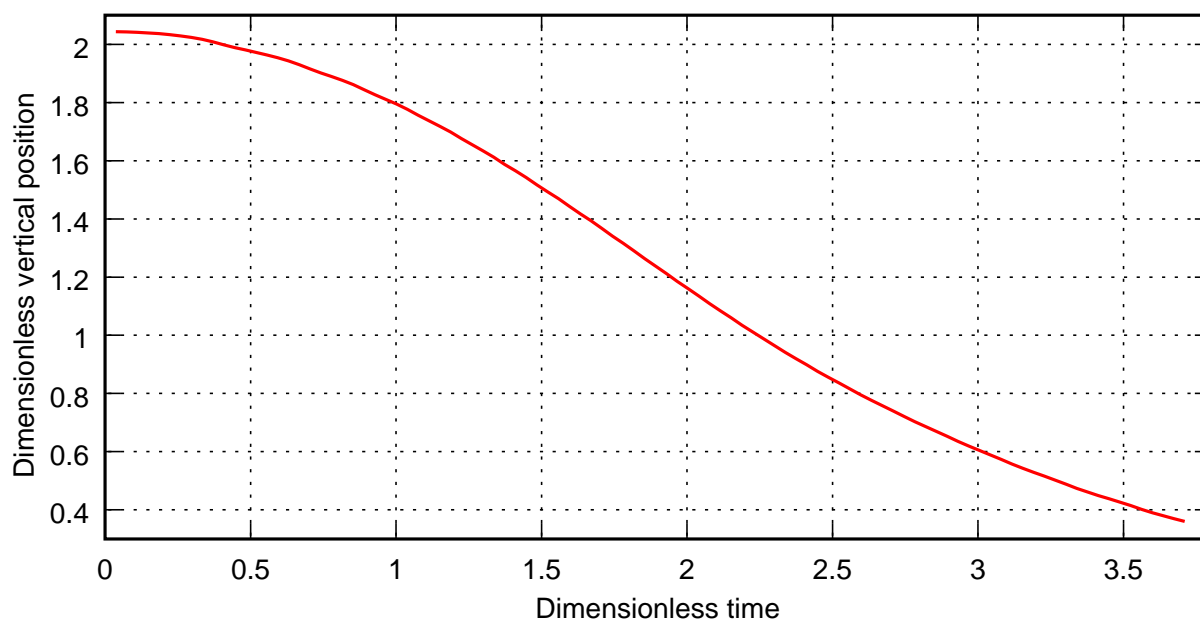


Figure 11: Dimensionless column height $h_c(t^*)/r_0$ versus dimensionless time $t^* = t\sqrt{2g/r_0}$ for the problem of the collapse of a cylindrical water column in 3D: numerical results.

resources as PETSc, MPICH, OpenDX, \LaTeX and JabRef.

REFERENCES

- Akin J.E., Tezduyar T.E., and Ungor M. Computation of flow problems with the mixed interface-tracking/interface-capturing technique (MITICT). *Computers & Fluids*, 36(1):2–11, 2007. doi:10.1016/j.compfluid.2005.07.008.
- Balay S., Buschelman K., Eijkhout V., Groppe W., Kaushik D., Knepley M., McInnes L., Smith B., and Zhang H. PETSc 2.3.0 users manual. Technical Report UC-405, Argonne Nat. Lab., 2005.
- Battaglia L. *Elementos finitos estabilizados para flujos con superficie libre: seguimiento y captura de interfase*. Ph.D. thesis, Facultad de Ingeniería y Ciencias Hídricas, Universidad Nacional del Litoral, 2009.
- Battaglia L., D' Elía J., Storti M.A., and Nigro N.M. Numerical simulation of transient free surface flows using a moving mesh technique. *ASME Journal of Applied Mechanics*, 73(6):1017–1025, 2006. doi:10.1115/1.2198246.
- Battaglia L., Storti M.A., and D' Elía J. Stabilized free surface flows. In S. Elaskar, E. Pilotta, and G. Torres, editors, *Mecánica Computacional*, volume XXVI, pages 1013–1030. 2007.
- Battaglia L., Storti M.A., and D' Elía J. An interface capturing finite element approach for free surface flows using unstructured grids. In Cardona, Storti, and Zuppa, editors, *Mecánica Computacional*, volume XXVII, pages 33–48. San Luis, 2008.
- Brooks A. and Hughes T.J.R. Streamline upwind/Petrov-Galerkin formulations for convection dominated flows with particular emphasis on the incompressible Navier-Stokes equations. *Computer Methods in Applied Mechanics Engineering*, 32(1-3):199–259, 1982. doi:10.1016/0045-7825(82)90071-8.
- Cruchaga M.A., Celentano D.J., and Breitkopf P. Modeling two-fluid interfaces for 3D flow problems. In Cardona, Storti, and Zuppa, editors, *Mecánica Computacional*, volume XXVII, pages 209–209. San Luis, 2008.

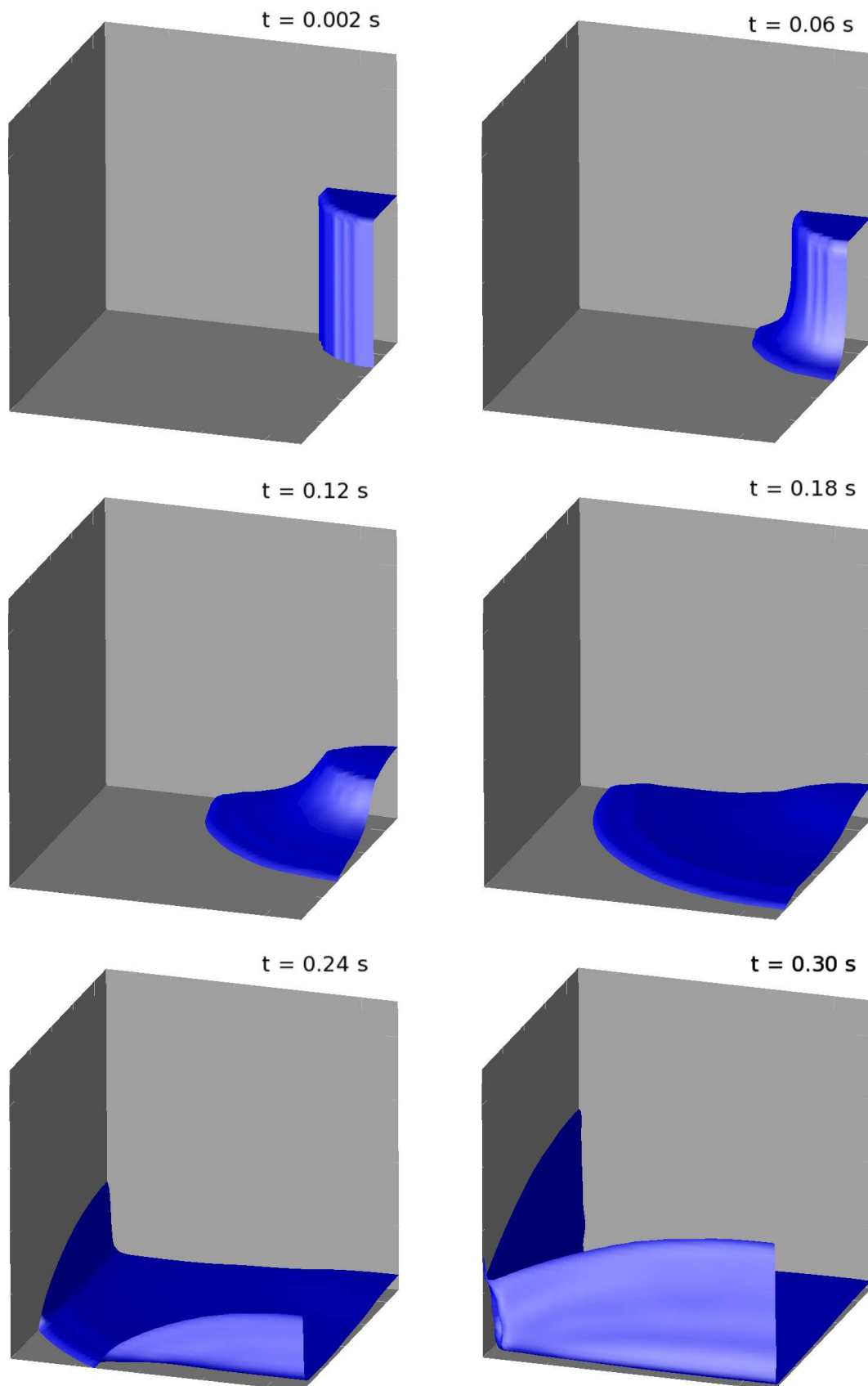


Figure 12: Initial stages for the problem of the collapse of a cylindrical water column in 3D.

- Cruchaga M.A., Celentano D.J., and Tezduyar T.E. Collapse of a liquid column: numerical simulation and experimental validation. *Computational Mechanics*, 39:453–476, 2007.
- Di Pietro D.A., Lo Forte S., and Parolini N. Mass preserving finite element implementations of the level set method. *Applied Numerical Mathematics*, 56(9):1179–1195, 2006.
- Elias R. and Coutinho A.L.G.A. Stabilized edge-based finite element simulation of free-surface flows. *International Journal for Numerical Methods in Fluids*, 54(6-8):965–993, 2007. doi: 10.1002/flid.1475.
- Enright D., Fedkiw R., Ferziger J., and Mitchell I. A hybrid particle level set method for improved interface capturing. *Journal of Computational Physics*, 183(1):83–116, 2002. doi: 10.1006/jcph.2002.7166.
- Gois J.P., Nakano A., Nonato L.G., and Buscaglia G.C. Front tracking with moving-least-squares surfaces. *Journal of Computational Physics*, 227(22):9643–9669, 2008. doi:10.1016/j.jcp.2008.07.013.
- Herrmann M. A balanced force refined level set grid method for two-phase flows on unstructured flow solver grids. *Journal of Computational Physics*, 227(4):2674–2706, 2008.
- Hirt C.W. and Nichols B.D. Volume of fluid (VOF) method for the dynamics of free boundaries. *Journal of Computational Physics*, 39(1):201–225, 1981. doi:10.1016/0021-9991(81)90145-5.
- Huerta A. and Liu W.K. Viscous flow with large free surface motion. *Computer Methods in Applied Mechanics and Engineering*, 69:277–324, 1988.
- Hughes T.J.R., Liu W.K., and Zimmermann T.K. Lagrangian-Eulerian finite element formulation for incompressible viscous flows. *Computer Methods in Applied Mechanics and Engineering*, 29(3):329–349, 1981. doi:10.1016/0045-7825(81)90049-9.
- Idelsohn S.R., Oñate E., and Del Pin F. The Particle Finite Element Method: a powerful tool to solve incompressible flows with free-surfaces and breaking waves. *International Journal for Numerical Methods in Engineering*, 61(7):964–984, 2004.
- LeVeque R.J. High-resolution conservative algorithms for advection in incompressible flow. *SIAM Journal on Numerical Analysis*, 33(2):627–665, 1996. doi:10.1137/0733033.
- Marchandise E. and Remacle J.F. A stabilized finite element method using a discontinuous level set approach for solving two phase incompressible flows. *Journal of Computational Physics*, 219(2):780–800, 2006.
- Martin J.C. and Moyce W.J. An experimental study of the collapse of liquid columns on a rigid horizontal plane. *Philosophical Transactions of the Royal Society of London. Series A, Mathematical and Physical Sciences*, 244(882):312–324, 1952. doi:10.1098/rsta.1952.0006.
- MPI. Message Passing Interface. <http://www.mpi-forum.org>, 2009.
- Mut F., Buscaglia G.C., and Dari E.A. New mass-conserving algorithm for level set redistancing on unstructured meshes. *Journal of Applied Mechanics*, 73(6):1011–1016, 2006.
- Olsson E. and Kreiss G. A conservative level set method for two phase flow. *Journal of Computational Physics*, 210(1):225–246, 2005. doi:10.1016/j.jcp.2005.04.007.
- Olsson E., Kreiss G., and Zahedi S. A conservative level set method for two phase flow II. *Journal of Computational Physics*, 225(1):785–807, 2007. doi:10.1016/j.jcp.2006.12.027.
- Osher S. and Sethian J.A. Fronts propagating with curvature-dependent speed: Algorithms based on Hamilton-Jacobi formulations. *Journal of Computational Physics*, 79(1):12–49, 1988. doi:10.1016/0021-9991(88)90002-2.
- PETSc-FEM. A general purpose, parallel, multi-physics FEM program. 2009. GNU General Public License (GPL), <http://www.cimec.org.ar/petscfem>.
- Rabier S. and Medale M. Computation of free surface flows with a projection FEM in a mov-

- ing mesh framework. *Computer Methods in Applied Mechanics and Engineering*, 192(41-42):4703–4721, 2003. doi:10.1016/S0045-7825(03)00456-0.
- Scardovelli R. and Zaleski S. Direct numerical simulation of free-surface and interfacial flow. *Annual Reviews in Fluid Mechanics*, 31:567–603, 1999.
- Sethian J.A. A fast marching level set method for monotonically advancing fronts. National Academy of Sciences, 1995.
- Shyy W., Udaykumar H.S., Rao M.M., and Smith R.W. *Computational Fluid Dynamics with Moving Boundaries*. Taylor and Francis, 1996.
- Sussman M. and Smereka P. Axisymmetric free boundary problems. *Journal of Fluid Mechanics*, 341:269–294, 1997.
- Tang B., Li J.F., and Wang T.S. Viscous flow with free surface motion by least square finite element method. *Applied Mathematics and Mechanics*, 29(7):943–952, 2008. doi:10.1007/s10483-008-0713-x.
- Tezduyar T.E. Interface-tracking and interface-capturing techniques for finite element computation of moving boundaries and interfaces. *Comp. Meth. in Appl. Mech. and Engr.*, 195(23-24):2983–3000, 2006. doi:10.1016/j.cma.2004.09.018.
- Tezduyar T.E., Mittal S., Ray S.E., and Shih R. Incompressible flow computations with stabilized bilinear and linear-equal-order interpolation velocity-pressure elements. *Computer Methods in Applied Mechanics and Engineering*, 95(2):221–242, 1992. doi:10.1016/0045-7825(92)90141-6.